Journal of the European Ceramic Society **19** (1999) 2941–2950
© 1999 Elsevier Science Ltd
Printed in Great Britain. All rights reserved
PII: S0955-2219(99)00058-8
0955-2219/99/$ - see front matter

Electrical Resistivity of Transition Metal Ion Doped Mullite

S. P. Chaudhuri, [a]* S. K. Patra [a] and A. K. Chakraborty [b]

[a]Special Ceramics Section, Central Glass and Ceramic Research Institute, Calcutta-700 032, India
[b]Instrumentation Section, Central Glass and Ceramic Research Institute, Calcutta-700 032, India

(Received 17 September 1998; accepted 21 February 1999)

Abstract

The electrical resistivity of pure mullite ($3Al_2O_3.2SiO_2$) varies from 10^{13} ohm-cm at room temperature (r.t.) to 10^4 ohm-cm at 1400 °C. It was observed that by doping mullite with the 3d-type transition metal ions, e.g. Mn, Fe, Cr and Ti, the resistivity of mullite could be reduced to 10^{11} ohm-cm, i.e. 1/100 that at r.t. and 1/5 that at 1400 °C. The resistivity of doped and undoped mullite decreased by 6–5 orders at about 500–600 °C but 4–3 orders between this temperature and 1400 °C. The 3d orbital electrons, the oxidation states and the concentration of the transition metal ions as well as the sites of mullite lattice occupied by the ions were found responsible for lowering of resistivity of mullite. Evidence of the presence of Mn^{2+}, Mn^{3+}, Fe^{3+}, Cr^{3+} and Ti^{4+} ions in mullite had been obtained which entered the octahedral site. The Ti^{4+} ion which substituted Al^{3+} ion in the octahedral site of mullite structure appeared to be the most efficient one to reduce the resistivity. This has been confirmed by the results of activation energy of resistivity/band gap energy, Eg which was the lowest for mullite doped with 1·0 wt% Ti^{4+} ion. At 1·0 wt% concentration level, these ions lowered the resistivity of mullite to minimum.
© 1999 Elsevier Science Ltd. All rights reserved

Keywords: resistivity, electrical conductivity, mullite, transition metal oxides.

1 Introduction

The electrical resistivity of mullite is high at room temperature and is approximately 10^{13} ohm-cm[1] which is well within the resistivity of insulators.[2] With the rise in temperature the resistivity of mullite dropped to 10^6 ohm-cm at 1000 °C and to 10^4 ohm-cm at 1400 °C.[3] It was calculated from these data that the band gap energy (Eg) of mullite is 1·43 ev.[4] The resistivity at about 1000 °C and the Eg value clearly suggested that mullite belongs to the semiconductor group of materials.

Mullite has an inherent defect structure which is better understood by comparing with the structure of sillimanite. The mullite and sillimanite structures are almost identical crystallographically and that the mullite-structure is derived from the sillimanite structure. While one hypothetical unit cell of mullite accommodates 3/4 of a molecule of mullite, i.e. 3/4 ($Al_2O_3{\cdot}2SiO_2$) or 4·5Al, 1·5Si and 9·75 O, a unit cell of sillimanite contains four molecules of sillimanite, i.e. 4($Al_2O_3.SiO_2$) or 8Al, 4Si and 20O. So, the mullite cell size is twice as big as the sillimanite cell size or four times the cell volume of mullite equals two times the cell volume of sillimanite.[5,6] Mullite ($Al_{18}Si_6O_{39} = 63$) and sillimanite ($Al_{16}Si_8O_{40} = 64$), having virtually same number of atoms in the same volume.

To derive mullite from sillimanite it is necessary to replace one (SiO_4) group in the sillimanite structure by one (AlO_4) group to obtain the mullite structure. This kind of replacement is possible in the sillimanite structure of the tetrahedral group of oxygens by putting one Al atom in the position of one Si atom and slightly pushing one oxygen atom from the centre of the group (Fig. 1).[7] Such displacement converts sillimanite ($Al_8Si_4O_{20}$) into $Al_9Si_3O_{20}$. But to maintain electroneutrality in the structure one oxygen atom should be removed from the structure whenever two Si atoms are replaced by two Al atoms. This mechanism of transformation of $Al_8Si_4O_{20}$ to $Al_9Si_3O_{19.5}$ can take place without any appreciable distortion in the structure.

Therefore, the same volume of sillimanite contains $Al_{32}Si_{16}O_{80}$ and mullite contains $Al_{36}Si_{12}O_{78}$ due to replacement of 4Si atoms by 4Al atoms and removal of 2O atoms from the structure of sillimanite.

* To whom correspondence should be addressed.

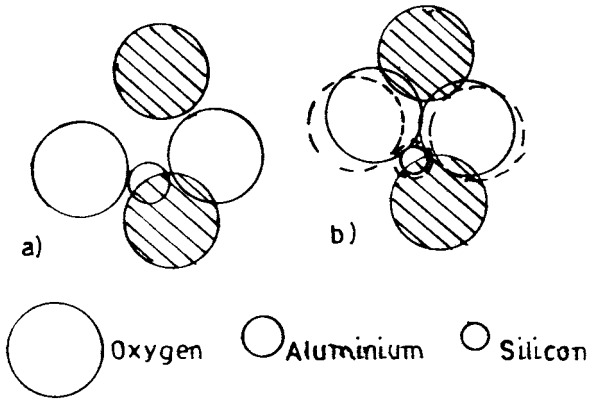

Fig. 1. (a) Grouping of oxygen atoms around Al atom in sillimanite. (b) Oxygen atoms in solid lines show actual grouping around Si atom and those in dotted line show slight displacement introduced in order to accommodate an Al atom in the position previously occupied by a Si atom, unshaded atoms lie in the reflection plane and shaded atoms lie above and below the reflection plane.[5]

The loss of oxygen atoms during formation of mullite leaves two vacant sites (oxygen or anion vacancy) in its unit cell. This implies that two holes exist in every 3/4 molecule of 3:2 mullite.

By high resolution electron microscopy (HREM) Epicier *et al.*[8] and Epicier[9] showed the existence of oxygen vacancy in the thin film (ca 30 Å) of mullite (Fig. 2).[9]

The mullite that forms by the replacement of Si^{4+} ion by Al^{3+} ion in the SiO_4 group of sillimanite structure has the stoichiometric composition, $3Al_2O_3.2SiO_2$. But several mullites of non-stoichiometric composition are possible due to further replacement of Si^{4+} by Al^{3+}. These compositions may be written by formulae (1) and (2) proposed by Dŭrovič[10] and Cameron,[11] respectively:

$$Al\left[Si_{2-x}Al_xO_{11/2} - x/2\right],\ 1{\cdot}25 \leq x \leq 1{\cdot}40 \qquad (1)$$

$$Al_2^{VI}[Al_{2+2x}Si_{2-2x}]^{IV}O_{10-x} \qquad (2)$$

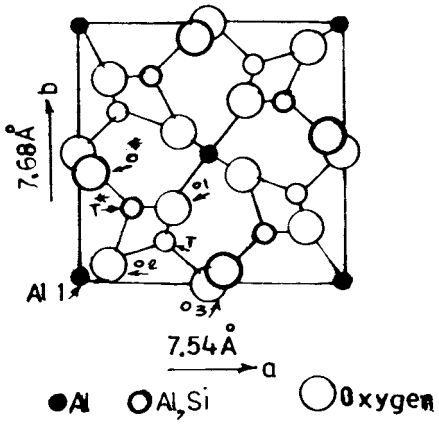

Fig. 2. Unit cell of mullite projected on (001) plane, oxygen vacancy exists along 03 type columns, and oxygen is shifted from thin walled (*T*) site to thick walled (*T**) site.[9]

and in (2) x denotes the number of oxygen atoms removed during the replacement process for charge balance.

The $3Al_2O_3.2SiO_2$ mullite lies at the centre of the series of mullite compositions derived from Dŭrovič's formula. But the $Al_2O_3.SiO_2$ mullite and $2Al_2O_3.SiO_2$ mullite are situated at the two terminals of this series. The series of mullite compositions has been extended further by Cameron and according to his formula a compound called iota alumina (ι-Al_2O_3) and synthesized by Foster[12] exists at the Al_2O_3 rich end of the series. This is a virtually SiO_2 free mullite. But at the other end $Al_2O_3.SiO_2$ lies as before.

The innumerable compositions of non-stoichiometric mullite and the stoichiometric mullite constitute a long series of isomorphous solid solutions of Al_2O_3 in mullite. These compositions arise due to the substitution of Si^{4+} ion by Al^{3+} ion in the tetrahedral site of mullite. Besides, substitution of Al^{3+} ion in the octahedral site of mullite by a host of metal ions, particularly of transition series, also takes place giving rise to solid solution of metals in mullite. The metal ions can be incorporated into mullite structure in different amounts and under different experimental conditions. The metal ions or dopants enter the structure of mullite to occupy the octahedral and tetrahedral sites, the channels formed by the chains of (AlO_6) groups along the c axis and tend to remain as clusters.

2 Brief Review of Work on Doped Mullite

Characterization of doped mullite had been the subject of many investigations. Concentrations of the dopants, oxidation states of the dopants and their positions in mullite structure were studied. The influence of the dopants on the changes that occurred in the mullite structure and also on the properties of mullite had been explored by several researchers. Most of the dopants belonged to the metals of transition series.

Murthy and Hummel[13] observed that mullite could hold up to 4 wt% TiO_2 at 1600°C, 12 wt% Fe_2O_3 at 1300°C and 10 wt% Cr_2O_3 at 1600°C in solid solution. Mullite also formed solid solutions with small amounts, i.e. 1·5 wt% V_2O_5 and 0·5 wt% MnO.[14] Non-transitional metal oxide dopants entered the mullite lattice in variable amounts, e.g. 41 wt% GeO_2,[15] 38 wt% Ga_2O_3,[15] 0·07 wt% ZrO_2[16] and 0·08 wt% Na_2O.[17]

The solid solubility of the dopants in mullite was found to be dependant on the temperature and atmosphere employed for incorporation of dopants and also on the oxidation state and size of the dopant cations. Mullite–Fe_2O_3 SS had 12 wt%

Fe_2O_3 at 1200°C[13] and only 1 wt% at 1750°C.[18] Decomposition of mullite occurred by the addition of excess dopants,[19,20] e.g. Fe_2O_3, Cr_2O_3 and TiO_2. Reducing atmosphere (low po_2) was shown to be unfavourable for inclusion of dopants due to distabilization of mullite structure and reduction of the dopant cation to lower oxidation state. Thus, the solubility of FeO (Fe^{2+}) in mullite was reduced to about 0·10 wt%.[21] The size of the cations is greater in their lower oxidation states and they are prevented from entering the mullite structure. This was observed with the dopants like transition metal ions.[14,21–23]

The unit cell dimensions (a, b, c) and the unit cell volume (C_V) of mullite suffered changes due to incorporation of dopants. Some authors[13–15,24] reported that these structural parameters of mullite increased irrespective of the nature of the dopents. But it was observed in another investigation[25] that the a axis of mullite showed contraction while the b and c axes expanded by doping it with transition metal ions. The Cr and Ti doped mullite suffered unit cell volume contraction. The small changes in the axial ratios, a/b and c/b, of the mullite lattice was a direct consequence of the variation in lattice parameters in the doped mullite.

The structural parameters a, b, c and C_V of the pure undoped mullite used by different investigators differed very little. A comparison of the results of different studies revealed that the a, b, c and C_V parameters of doped mullites had significant variation with respect to those of undoped pure mullite.

The maximum and minimum values of a, b, c and C_V of pure and doped mullites are compiled in Table 1.

The change in the shape of mullite doped with the transition metal ions was studied.[25] It was established that the shape of mullite crystals was influenced by the dopant ions because the lattice parameters a, b, c expanded or contracted due to their incorporation in the lattice. The authors[25] showed that while b and c axes increased steadily contraction took place along a axis. The resultant change along a and b axes, was compared with the change along c axis. The large increase in the c axis of Fe and Ti doped mullites was the reason for their stout needle shape. The rectangular shape of the Mn doped mullite was due to moderately greater increase of its c axis but the decrease in the c dimension of the Cr-doped mullite explained its spheroidal shape.

The effect of dopants on the size of mullite crystals was found to be variable.[25] When incorporated into pure mullite the dopants like Mn and Cr increased its size but the dopants like Fe and Ti decreased its size. The expansion of unit cell volume of mullite by Mn and Cr but the contraction of unit cell volume of mullite by Fe and Ti matched well the results of the size of the mullite crystals doped with the respective dopants.

Introduction of dopants in the mullite structure caused significant change in its properties. Both the density and refractive index of mullite diminished by incorporating Al_2O_3 into it when Al^{3+} substituted Si^{4+} in the tetrahedral site.[10,11] Refractive index of Fe_2O_3 doped mullite increased with the concentration of Fe_2O_3[26] and density of GeO_2 doped mullite rose with the rise in GeO_2 content.[15] Fe^{3+} replaced Al^{3+} in the octahedral site and Ge^{4+} replaced Si^{4+} in the tetrahedral site of mullite. Fe_2O_3[27–29] imparted red to black colour in mullite due to 3–18 mol% Fe_2O_3 in solid solution. The density, flexural strength and fracture toughness of ZrO_2 doped mullite were found to be much higher than those of the undoped mullite.[30–32] A continuous solid solution of 15 vol% ZrO_2 with mullite was attributed to the enhancement of these properties.

Very little attention was paid to the electrical properties of mullite. The electrical resistivity[3] and the dielectric loss angle, $\tan\delta$[33] of pure mullite (3 $Al_2O_3.2SiO_2$) were reported in the literature. Saalfeld and Guse[34] studied electrical resistivity of pure mullite (2 $Al_2O_3.SiO_2$). The results showed that the

Table 1. Range of values of unit cell parameters (a,b,c and C_v) of pure (undoped) and doped mullite samples[a]

Sample	a (Å)	b (Å)	c (Å)	C_V (Å)^3
Mullite	7·544–7·560	7·687–7·690	2·881–2·886	167·07–167·62
(pure undoped)	(7.545)	(7.687)	(2.886)	(167·38)
Mullite	7·527–7·563	7·687–7·721	2·883–2·890	167·30–168·33
(Mn-doped)	(7·527–7·553)	(7·687–6·699)	(2·887–2·890)	(167·30–167·77)
Mullite	7·532–7·588	7·682–7·730	2·884–2·900	167·03–170·08
(Fe-doped)	(7·532–7·544)	(7.682–7.698)	(2·884–2·893)	(167·03–167·88)
Mullite	7·538–7·571	7·692–7·712	2·884–2·903	167·08–169·43
(Cr-doped)	(7·538–7·538)	(7·691–7·705)	(2·884–2·887)	(167·08–167·46)
Mullite	7·535–7·578	7·535–7·703	2·887–2·897	167·33–168·85
(Ti-doped)	(7·535–7·539)	(7·686–7·695)	(2·889–2·890)	(167·33–167·57)

[a]Note: Values without parentheses are based on as many references as possible; values within parentheses are based on the authors' work.[25]

3 $Al_2O_3.2SiO_2$ mullite obtained by sintering SiO_2 and Al_2O_3 mixture had energy band gap of 1·43 ev.[4] whereas the $2Al_2O_3.SiO_2$ mullite grown from the fused SiO_2 and Al_2O_3 melt had an energy band gap of 7·7 ev.[34]

The fused (melt grown) 2:1 mullite is, therefore, a good electrical insulator comparable to SiO_2 and Al_2O_3 but the sintered 3:2 mullite is a potential electrical conductor. Also, the 2:1 mullite does not allow any foreign cation to enter its structure but the 3:2 mullite accommodates a large number of foreign cations in its structure by way of formation of solid solution, cluster formation and in the structural channels.

It appears from the survey of literature that no attempt has yet been made to take advantage of solid solubility of various cations in different concentrations in the structure of 3:2 mullite to reduce its electrical resistivity. One and only one study on the electrical resistivity of 3:2 mullite doped with the metal ions has been reported[35] by the first author of the present paper and his group.

3 Principle

The incorporation of metal ions occurs mostly in the (AlO_6) octahedral chains in mullite by the replacement of Al^{3+} ion by M^{n+} ion. Three situations may arise due to the substitution process, e.g. excess and deficit of one electron will occur in the mullite structure if $n > 3$ and $n < 3$. respectively. However, electroneutrality of the structure is maintained when $n = 3$.

If $n = 3$ and M is a 3d transition metal ion with X electrons in its d-orbitals so that X varies from 1 to 3 and 6 to 8 and it substitutes Al^{3+} ion which has no 3d electron, some labile 3d electrons remain in the mullite structure. In other cases, i.e. $n \neq 3$, if M substitutes Al^{3+} ion with no 3d electron so that excess electron or hole is generated in the mullite structure, X may range from 1 to 10.

The entry of 3d electrons and the formation of excess electrons or holes in the mullite structure due to such substitution process are the main reasons for the decrease of electrical resistivity of the transition metal ion doped mullite.

Apart from the effects of inherent oxygen-ion vacancy and the induced electron and hole on the reduction of the electrical resistivity of doped mullite, the transition metal ions that occupy the interstitial positions and structural channels as well as that exist in the form of clusters in the structure of mullite also influence its resistivity.

Therefore, the electrical resistivity of mullite ($3Al_2O_3.2SiO_2$), undoped and doped with 3d transition metal ions, e.g. Mn, Fe, Cr and Ti has been measured from room temperature to 1400 °C. The changes in electrical resistivity of mullite due to doping are explained on the basis of such characteristics of the dopant ions as the oxidation states, electronic configuration and incorporation into mullite lattice sites. The present paper embodies the report of this investigation.

4 Experimental Procedure

4.1 Sample preparation

Very pure mullite ($3Al_2O_3.2SiO_2$) was prepared by co-precipitation from solution of analytical reagent (AR) grade Al $(NO_3)_3.9H_2O$ and $Si(OC_2H_5)_4$ by analytical reagent grade NH_4OH. Each of the four dopant ions, Mn^{2+}, Fe^{3+}, Cr^{3+} and Ti^{4+}, was incorporated into mullite during the co-precipitation stage by mixing their analytical reagent grade inorganic or organometallic salt solutions with the aluminium nitrate and tetraethyl silicate solutions. The co-precipitates, after washing and drying, were calcined at 500 °C for 3 h to yield reactive mullite precursors. Discs were then pressed from the precursors at ca 300 MPa and sintered at 1600°C for 3 h. The preparation of sample was described in details elsewhere.[25]

4.2 Sample characterisation

The sample was chemically analysed by the standard wet chemical method and was found to contain only Al_2O_3 and SiO_2 in the 3:2 molar proportion, i.e. this mullite was stoichiometric or 3:2 variety. The bulk density and apparent porosity of the samples were calculated from their dimension, weight and density of solid.

The X-ray diffraction (XRD) pattern of the prepared sample showed that it contained only one phase, i.e. mullite ($3Al_2O_3.2SiO_2$) and no other phase could be detected.

The concentration of each dopant ion incorporated into mullite was checked by the chemical analysis and also by the X-ray flurescence (XRF) technique.[25] Both these methods confirmed that mullite contained almost the same amount of the ion as that added to it.

The unit cell dimensions and the unit cell volume of the undoped and doped mullite samples were measured by the X-ray diffractometry.[25] The change in the volume of the unit cell of doped mullite suggested that the dopant ions enter the mullite structure in solid solution.

The incorporation of the dopant ions into the mullite lattice was investigated by Chaudhuri and Patra[36] with the help of electron paramagnic resonance (EPR) and Mössbauer spectroscopy supplemented by X-ray diffractometry of the doped mullites.

The EPR spectrum of a doped mullite sample exhibited a number of signals with their g_{eff} (effective g) values and line widths, ΔH_{PP}, [$g_{eff} = h\nu/\beta H$; Plank constant (h), microwave frequency (ν), Bohrmagneton (β), external field (H)] There were two signals at $g_{eff} = 2{\cdot}0$ and $1{\cdot}9$ with their $\Delta H_{PP} = 300-475$ Gauss for Mn doped mullites; three signals at $g_{eff} = 2{\cdot}1$, $4{\cdot}2$ and $5{\cdot}1$ with their $\Delta H_{PP} = 100-200$ Gauss for Fe doped mullites and two signals at $g_{eff} = 2{\cdot}5$ and $5{\cdot}0$ with their $\Delta H_{PP} = 160-240$ Gauss for Cr doped mullites. There were no EPR spectra of the Ti-doped mullites.

These EPR signals with the characteristic g_{eff} values and line widths, ΔH_{PP} provided evidence for the presence of paramagnetic ionic species of the transition metal ions. i.e. Mn, Fe and Cr in the mullite lattice. The signal at $g_{eff} = 2{\cdot}0$ with no hyperfine structure indicated that Mn^{2+} ion was present as cluster and the signal at $g_{eff} = 1{\cdot}9$ showed that Mn^{3+} ion occupied the octahedral site in mullite. All the three signals of Fe doped mullites, suggested the existence of only Fe^{3+} ion in mullite. That Fe^{3+} ion occupied the octahedral site of mullite was justified by the appearance of signals at $g_{eff} = 4{\cdot}2$ and $g_{eff} = 5{\cdot}1$, but the signal at $g_{eff} = 2{\cdot}1$ was assigned to Fe^{3+} ion clusters in mullite. Both the signals of Cr-doped mullite were due to Cr^{3+} ion. The signal at $g_{eff} = 5{\cdot}0$ confirmed that Cr^{3+} ion entered the octahedral site of mullite but the inclusion of Cr^{3+} ion in the interstitial lattice position was shown by the signal at $g_{eff} = 2{\cdot}5$. The absence of EPR signal in Ti-doped mullite was a strong evidence of the presence of only non-paramagnetic Ti^{4+} ion which occupied the octahedral position of the mullite lattice.

More evidence was gathered from the Mössbauer spectrum of Fe doped mullite sample. Analysis of the two broad symmetric lines in the spectrum[36] by the two doublet as well as one doublet schemes of fitting yielded large values of isomer shift (IS$\approx$0·30) and quadrupole splitting (QS$\approx$1·15). The large IS was appropriate for the existence of only Fe^{3+} ion which substituted Al^{3+} ion in the octahedral site of mullite structure.

The measurement of lattice parameter of Cr doped mullite by X-ray diffractometry showed that the b-axis expanded more than the a-axis in these samples of low Cr content.[25] This fact stood as further evidence of the presence of only Cr^{3+} ion in these samples and that Cr^{3+} ion replaced Al^{3+} ion in the octahedral site.[37–40].

The observation of the fractured and HF etched surfaces of mullite doped with the transition metal ions by SEM revealed that the mullite grains were well sintered and closely packed.[25] The existence of doping agents in the periphery of the mullite grains and in the grain boundaries could not be identified from the EDAX profile of the grain boundaries of the doped mullite samples. Therefore, the doping agents had not segregated at the grain boundaries. A few electron micrographs of the mullite samples taken in SEM are exhibited in Fig. 3(a)–(e).

4.3 Measurement of electrical resistivity

The fired discs were ground and polished to 20–25 mm dia and 3–4 mm thick. Both sides of the discs were coated with a platinum paste and fired at 1000 °C for 15 min to deposit the metallic platinum.

4.3.1 At room temperature

The platinum coated disc was placed in a press-contact type teflon holder to minimize leakage resistance from the holder. The assembly was then placed inside a vacuum chamber which was evacuated to ca 10^{-2} m.bar. The vacuum chamber was properly shielded and the length of the coaxial cable connecting the electrometer and the sample was kept as short as possible to minimise the electromagnetic and the radio frequency interferences.

A high input resistance (R_1) was included in the circuit in series. It was variable within different ranges and was provided for by the electrometer. A constant DC voltage (V) of about 1·5 volts was applied from a battery across the sample. The voltage (V_1) across the input resistance was measured by the electrometer. Thus, current (I) in the circuit was $I = V_1/R_1$. So, the resistance (R) of the sample was calculated as

$$R = V/I \tag{3}$$

Before the measurement of resistance of each sample the voltage of the battery was checked against a DC micro-voltmeter of sensitivity 100 μV. The resistivity (ρ) of the sample was then calculated by the relationship

$$\rho = R(A/\ell) \tag{4}$$

where R, A and ℓ are resistance, area and thickness of the sample.

4.3.2 At higher temperature

Thin (0·2 mm) platinum were was spot welded by electric discharge with the platinum coated surfaces of the disc and suspended at the centre of a small electrically heated furnace (up to 1500°C). The platinum lead wires coming out of the furnace were connected to a specially designed instrument to measure resistance of sample in the range of 10^2–10^8 Ohm.

A constant voltage was supplied to the sample from a source. A high impedence amplifier provided

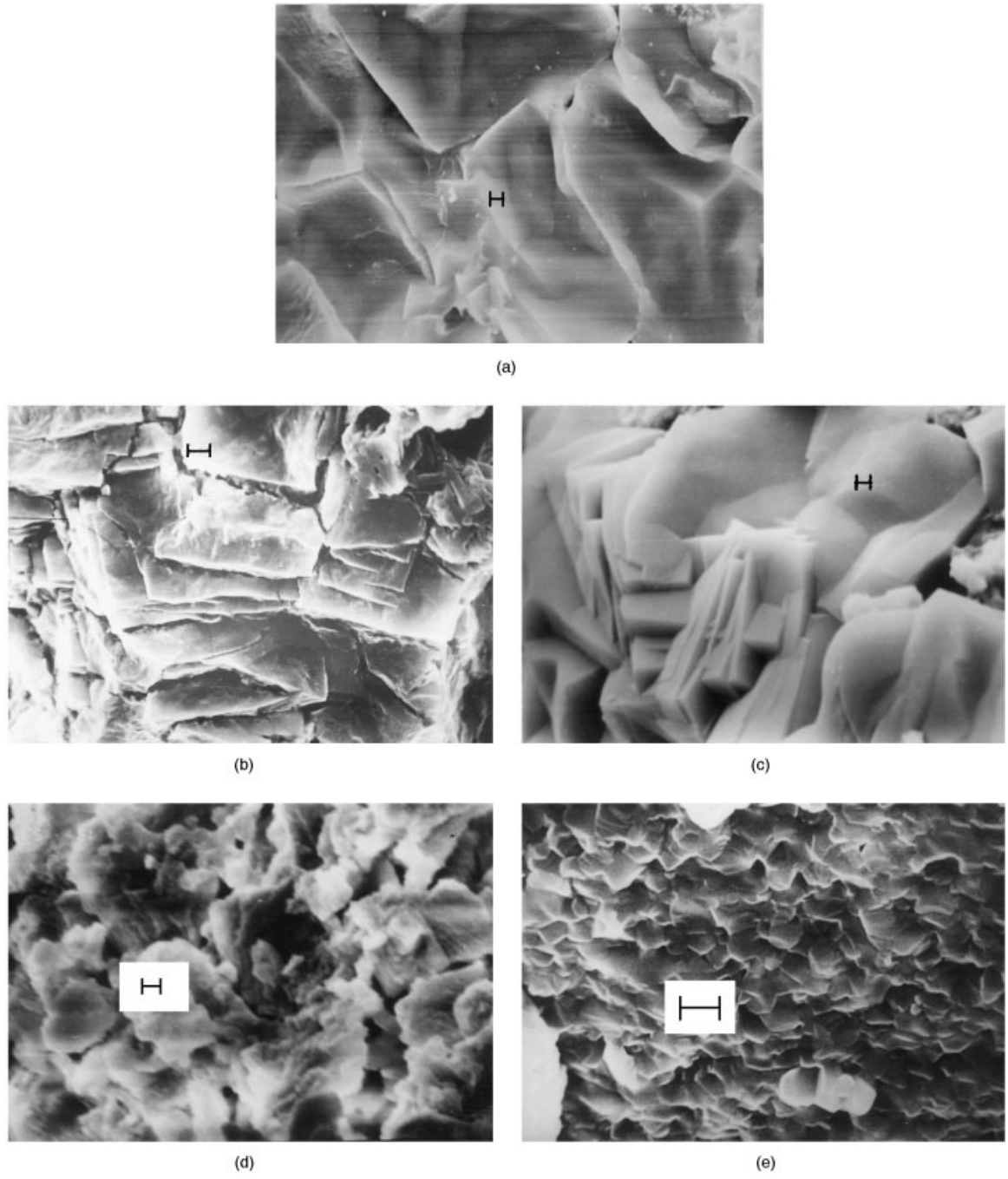

Fig. 3. Scanning electron micrographs of undoped and doped (2 wt% ion) mullite samples: (a) undoped; (b) Mn-doped; (c) Fe-doped; (d) Cr-doped; (e) Ti-doped (Bar = 1 μm).

the output voltage proportional to the resistance of the sample. This output voltage was fed to the Digital Panel Meter (DPM) amplifier as well as the amplifier for the X-T recorder.

The DPM showed directly the sample resistance at any temperature but the recorder traced the curve on the strip chart showing continuous change of sample resistance with temperature. The recorder was calibrated for full scale pen deflection on the chart paper at different sensitivities against the standard resistances. Calibration curves of pen displacement versus standard resistance were drawn and from the known pen displacement at any temperature the sample resistance at the temperature was computed from the calibration curves. The electrical resistivity (ρ) of the sample was calculated as before.

4.3.3 Determination of activation energy

The temperature dependence of electrical resistivity of the samples is expressed by the Arrhenius type equation as follows:

$$\rho = \rho_o \exp(Eg/2KT) \tag{5}$$

where ρ and ρ_o are resistivity of samples at any temperature and 0°C, respectively. E, K and T are activation energy, Boltzman constant ($8{\cdot}62\times 10^{-5}$ eV) and absolute temperatures, respectively.

A plot of $\log_{10}\rho$ versus $1/T$ was drawn for each sample between room temperature and 1400 °C at 100°C intervals. The activation energy of electrical resistivity of the sample was calculated in eV unit from the slope of the plot as follows:

$$Eg = \text{slope} \times 4{\cdot}606 \times 8{\cdot}62 \times 10^{-5}\,\text{eV} \quad (6)$$

5 Results

The electrical resistivity, activation energy and % theoretical density of undoped and 0·5–2·0 wt% of each of Mn, Fe, Cr and Ti doped mullite samples are presented in Table 2. The performance of the dopants varied with temperature and concentration. The temperature dependence of resistivity due to doping of mullite with the above metal ions is shows in Fig. 4. The effect of the entire temperature range (room temp. 1400°C) on the resistivity was obtained by calculating activation energy of resistivity (*Eg*) from these plots and they are included in Table 2. The variation of Eg with the concentration of each dopant is displayed in Fig. 5. The overall performance of each dopant at equal concentration level to lower the electrical resistivity of mullite may be clearly understood from Table 2 and Fig. 5. The Ti appeared to be the most efficient and the Fe was the least but both Mn and Cr were superior to Fe and inferior to Ti. The dopants were most effective when added to the extent of 1·0 wt% in mullite. The Eg of 1·0 wt% Ti doped mullite dropped below 1·0 eV. (i.e. 0·97 eV).

The electrical resistivity of undoped and 1·0 wt% metal ion doped mullite was plotted against temp. in Fig. 6. Two salient points emerged from this figure. The temperatures at which the resistivity of the doped mullites reached 10^6 ohm-cm order (700–900°C) were 200–400°C less than that (1100°C) at which the resistivity of undoped mullite attained the same order. The fall of resistivity approached constant rate at about 450 °C for undoped mullite but within 500–600°C for doped mullites.

The oxidation states and the electronic configurations of the transition metal ions as well as the mullite lattice sites occupied by them are tabulated in Table 3. The dopant ions preferred to enter the octahedral site only with the exception that Mn^{2+} and Cr^{3+} ion were found to exist in cluster and in the channels created by AlO_6 octahedra.

6 Discussion

At room temperature the electrical resistivity of undoped pure mullite was of the order of 10^{13} ohm-cm[1] and that of the doped mullite was of the order of 10^{11} ohm-cm.[35] At 1400°C the doped mullite showed resistivity of the order of 10^4 ohm-cm (Table 2). So, the incorporation of the transition metal ions, the dopants, alone could reduce the electrical resistivity of mullite by two orders of magnitude at room temperature (ca 30°C). At room temperature therefore, the resistivity of doped mullite was (1/100) of the resistivity of undoped mullite and at 1400°C the resistivity of doped mullite was (1/5) of the resistivity of undoped mullite (Table 2).

Table 2. Description, electrical resistivity, activation energy and % theoretical density of pure (undoped) and doped mullite samples

Sample no.	*Description*	*Electrical resistivity* (ρ) *(ohm-cm) at*		*Activation energy* (E_g)	*% Theoretical density*
		500°c	*1400°c*	*eV*	
1.	Mullite (pure, undoped)	$1{\cdot}38\times10^8$	$6{\cdot}46\times10^4$	1·44	50·80
	Mullite + Mn (wt%)				
2.	0·5	$1{\cdot}23\times10^8$	$3{\cdot}09\times10^4$	1·42	70·96
3.	1·0	$1{\cdot}28\times10^8$	$1{\cdot}46\times10^4$	1·13	66·92
4.	1·5	$0{\cdot}54\times10^8$	$1{\cdot}26\times10^4$	1·25	73·30
5.	2·0	$0{\cdot}62\times10^8$	$1{\cdot}26\times10^4$	1·34	66·41
	Mullite + Fe (wt%)				
6.	0·5	$0{\cdot}28\times10^8$	$4{\cdot}07\times10^4$	1·42	57·95
7.	1·0	$0{\cdot}06\times10^8$	$2{\cdot}14\times10^4$	1·27	61·83
8.	1·5	$0{\cdot}17\times10^8$	$2{\cdot}88\times10^4$	1·30	64·06
9.	2·0	$0{\cdot}14\times10^8$	$3{\cdot}2\times10^4$	1·37	62·04
	Mullite + Cr (wt%)				
10.	0·5	$0{\cdot}17\times10^8$	$7{\cdot}24\times10^4$	1·23	57·38
11.	1·0	$0{\cdot}17\times10^8$	$5{\cdot}01\times10^4$	1·17	57·04
12.	1·5	$0{\cdot}79\times10^8$	$2{\cdot}57\times10^4$	1·37	58·32
13.	2·0	$1{\cdot}09\times10^8$	$6{\cdot}31\times10^4$	1·26	60·94
	Mullite + Ti (wt%)				
14.	0·5	$0{\cdot}25\times10^8$	$1{\cdot}20\times10^4$	1·10	59·08
15.	1·0	$0{\cdot}07\times10^8$	$6{\cdot}03\times10^4$	0·97	65·32
16.	1·5	$0{\cdot}15\times10^8$	$3{\cdot}02\times10^4$	1·35	63·72
17.	2·0	$0{\cdot}08\times10^8$	$2{\cdot}75\times10^4$	1·19	71·00

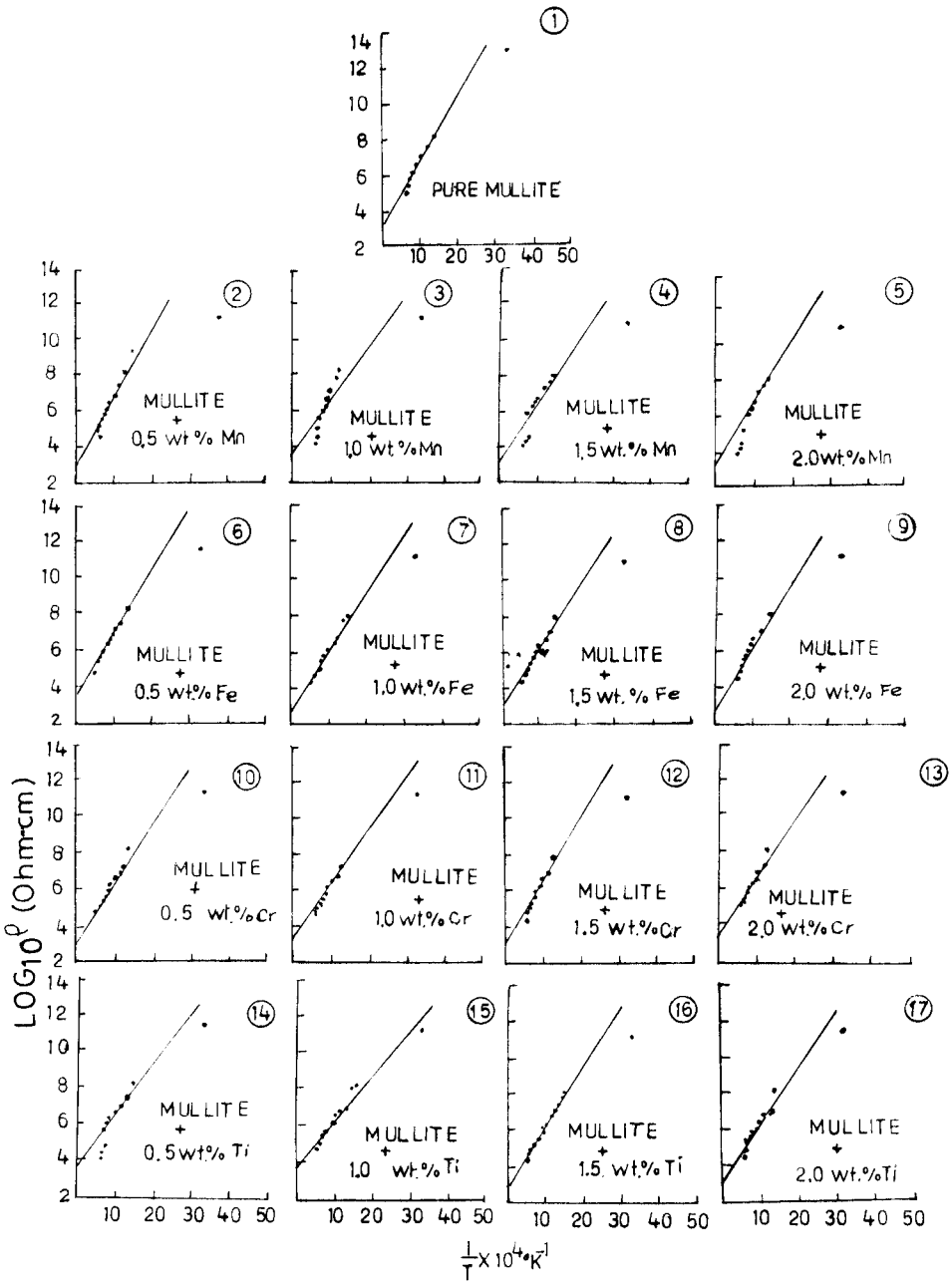

Fig. 4. Arrhenius plots ($\log_{10}\rho - 1/T$) of undoped (pure) and doped (Mn, Fe, Cr, Ti ions) mullite samples.

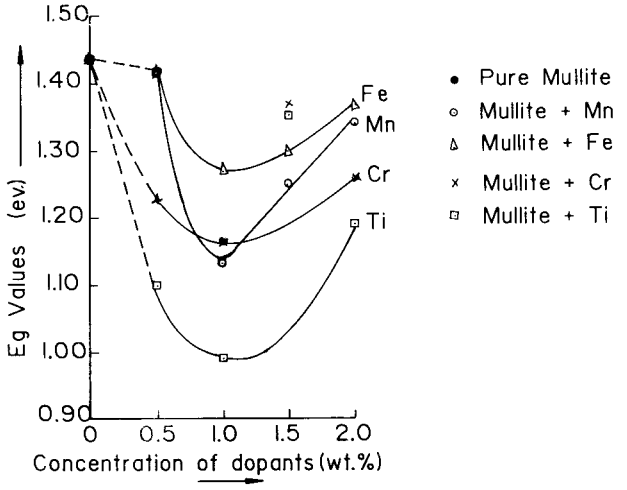

Fig. 5. Dependance of Eg of doped mullite samples on the concentration of the dopant ions (Mn, Fe, Cr, Ti).

This implied that the rate of decrease of resistivity of mullite was higher at low temperature than that at elevated temperature. So far as the electrical resistivity (or conductivity) is considered, the behaviour of mullite in this respect was parallel to that of non-metals.[41]

It is also interesting to note that doping mullite by the transition metal ions could lower the temperature at which pure mullite attained the resistivity of the semiconductor type material (i.e. 10^6ohm-cm) by about 200–400°C (i.e. 900–700°C).

The transition metal ions, e.g. Mn^{2+}, Fe^{3+}, Cr^{3+} and Ti^{4+} entered the mullite lattice in different positions and substituted Al^{3+} ion. It was shown[36] by EPR and Mössbauer spectroscopy that these ions can exist in more than one oxidation state and occupied octahedral sites and also the

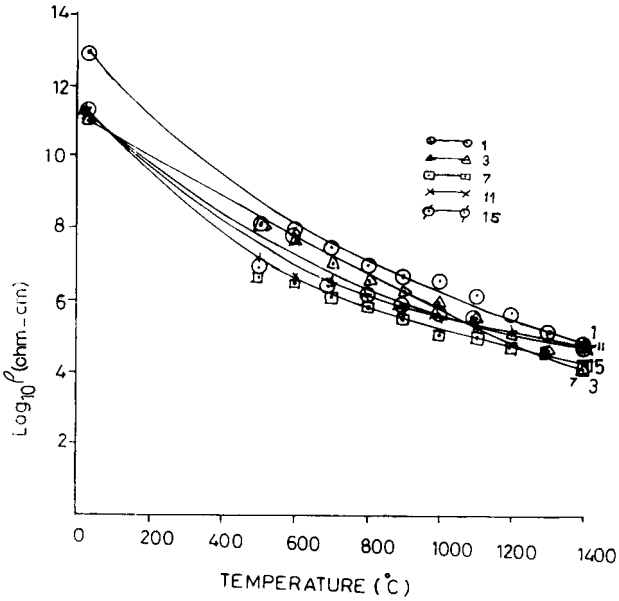

Fig. 6. Relationship between electrical resistivity of undoped and 1·0 wt% ion doped mullite samples and temperature.

Table 3. Electronic configurations, oxidation states of dopant ions and their positions in mullite

Transition metal ions	*Electronic configurations*	*Valency state*	*Positions occupied in mullite structure*
Mn	[Ar] $3d^5$ 4S°	2+	Cluster
Mn	[Ar] $3d^4$ 4S°	3+	Octahedral
Fe	[Ar] $3d^5$ 4S°	3+	Octahedral
Cr	[Ar] $3d^3$ 4S°	3+	Octahedral, channel
Ti	[Ar] 3d° 4S°	4+	Octahedral

structural channels in mullite. The Mn ion remained partly in the Mn^{3+} state in the octahedral site. The Fe and Cr ions occurred in the Fe^{3+} and Cr^{3+} state, respectively, Fe^{3+} ion being in the octahedral site and Cr^{3+} in the octahedral site and in the interstitials. But Ti ion entered the octahedral site only as the Ti^{4+} ion. This resulted in entry of Mn^{3+}, Fe^{3+}, Cr^{3+}, Ti^{4+} ions having 3d electrons in the mullite structure in place of Al^{3+} ion which has no 3d electrons. Besides, Mn^{2+} ions with 3d electrons were also present in the structure. The local electron density in the mullite structure, therefore, increased and the resistivity of doped mullite decreased significantly even at room temperature. This effect of doping mullite with the 3d type transition metal ion on its resistivity was demonstrated in a previous work[35] by determining the position annihilation lifetime (PAL) and 'S' parameter by PAL spectroscopy and doppler broadened annihilation radiation line shape analysis (DBARLA), respectively.

The resistivity of doped mullite samples dropped with temp. more than that of undoped mullite samples. This was probably caused by the enhanced mobility at higher temperature of electrons and ions present in their structure. At 1400°C the resistivity of doped mullites, of course, decreased to a larger extent than the undoped mullite. However, the rate of fall of resistivity of doped and undoped mullite slowed down with temperature but less so for the doped mullite. This is revealed from the plots shown in Fig. 6. It appears that the resistivity of the undoped and doped mullite samples decreased quickly (5–6 orders) from room temp. up to 450–600°C and then slowly (4–3 orders) to 1400°C and above. Mullite samples, therefore behaved like non metallic electrical conductors because their conductivity rises faster at lower temperature but slows down at higher temperature.

The relative efficiency of the dopant ions to diminish the electrical resistivity of mullite may be estimated from the Eg values of the samples presented in Table 2 and Fig. 5. Among the four dopants tried the Ti^{4+} ion appeared to be the most efficient. The Fe^{3+} ion was the least efficient but the Mn^{2+} and Cr^{3+} ions stood in between. Irrespective of the nature of the dopant the efficiency was dependant on the concentration of the dopant ions and it reached maximum at 1·0 wt%. This is evident from the lowest Eg for each ion at 1·0 wt% concentration (Table 2). Any fluctuation in the concentration level of ions caused rise in the Eg and consequent fall in the efficiency.

The substitution of Al^{3+} ion in the mullite lattice by Fe^{3+}, Cr^{3+} or Mn^{3+} ion does not disturb its electroneutrality. The $3d^5$ electronic configuration of Fe^{3+} ion is more stable than the $3d^4$ and $3d^3$ electronic configuration of Mn^{3+} and Cr^{3+} ions, respectively.[42] This made Fe^{3+} ion less effective to reduce the electrical resistivity compared to other ions. Creation of a very fast electron or formation of a hole is possible when Al^{3+} ion is replaced by Ti^{4+} ion or Mn^{2+} ion in the mullite structure. However, it was observed[36] that Mn^{2+} ion could not substitute Al^{3+} ion in mullite but remained there as cluster. This evidence suggested that the formation of hole had not taken place in the Mn doped mullite. Both the Mn^{3+} ion and a fraction of Cr^{3+} ion occupied the octahedral position in mullite. Aside from this, Mn^{2+} ion existed as cluster and Cr^{3+} ion occurred in the interstitial. So Cr^{3+} and Mn^{3+}/Mn^{2+} ions were almost equally efficient to bring down the electrical resistivity of mullite. Therefore, only in the Ti-doped mullite very fast electron was released from the valence band which jumped into the donar level and this was probably responsible for maximum lowering of resistivity and the lowest Eg value of the Ti-doped mullite at almost all concentration level of Ti ion (Table 2).

7 Conclusions

The investigation of electrical resistivity of transition metal ion doped mullite has led to the following conclusions.

1. The electrical resistivity of transition metal ion (Mn^{2+}, Fe^{3+}, Cr^{3+} and Ti^{4+}) doped mullite was 1/100 (i.e. two order less) at room temp. and 1/5 at 1400°C of that of pure (undoped) mullite.
2. The efficiency of the dopants to lower the electrical resistivity of pure (undoped) mullite was maximum with Ti^{4+} ion and minimum with Fe^{3+} ion but intermediate with Mn^{2+} and Cr^{3+} ions.
3. 1·0 wt% of a transition metal ion was required to dope pure mullite to achieve maximum lowering of its electrical resistivity.
4. The electronic configuration of 3d orbital and oxidation state of a transition metal ion were very important factors to lower electrical resistivity of mullite, the oxidation state playing the key role.
5. A dopant ion in more than trivalent state when substituted Al^{3+} ion in the octahedral site of mullite resulted in maximum drop in electrical resistivity.

Acknowledgements

One of the authors, S. K. Patra, wishes to thank the Council of Scientific and Industrial Research, India for a financial grant of Senior Research Fellowship to carry out this work.

References

1. Buchanan, R. C., In *Ceramic Materials for Electronics*, ed. R. C. Buchanan. Mercel Dekker, New York, 1990, pp. 1–71.
2. Van Vlack, L. H., *A Text Book of Materials Technology*. Addison–Wesley, Reading, MA, 1973, pp. 270–292.
3. Bárta, R. and Bártuska, M., Mullite studies. *Tech. Sil.*, 1957, **4**, 146–185.
4. Chaudhuri, S. P., Bandopadhyay, S. and Mitra, N., Electrical resistivity of mullite prepared by sintering $SiO_2 + Al_2O_3$ mixtures. *Interceram.*, 1995, **44**(5), 300–306.
5. Wyckoff, R. W. G., Greig, J. W. and Bowen, N. L., X-ray diffraction patterns of mullite and of sillimanite. *Am. J. Sci.*, 1926, **11**(66), 460–472.
6. Taylor, W. H., Structure of sillimanite and related materials. *J. Soc. Glass. Tech.*, 1932, **16**, 111 T–120 T.
7. Taylor, W. H., The structure of sillimanite and mullite. *Z. Krist.*, 1928, **689**, 503–521.
8. Epicier, T., Benefits of high resolution electron microscopy for the structural characterisation of mullite. *J. Am. Ceram. Soc.*, 1991, **74**(10), 2359–2366.
9. Epicier, T., O'Keefe, M. A. and Thomas, G., Atomic imaging of 3:2 mullite. *Acta Crystallogr., Sect-A, Cryst. Phys. Diffr., Theo. Gen. Crystallogr.*, 1990, **A46**, 948–962.
10. Dŭrovič, S., Isomorphism between sillimanite and mullite. *J. Am. Ceram. Soc.*, 1962, **45**(4), 157–161.
11. Cameron, W. E., Mullite: a substituted alumina. *Am. Min.*, 1977, **62**, 747–755.
12. Foster Jr, P. A., Nature of alumina in quenched cryolite alumina melts. *J. Electrochem. Soc.*, 1959, **106**, 971–975.
13. Murthy, M. K. and Hummel, F. A., X-ray study of the solid solution of TiO_2, Fe_2O_3 and Cr_2O_3 in mullite ($3Al_2O_3.2SiO_2$). *J. Am. Ceram. Soc.*, 1960, **43**(5), 267–273.
14. Schneider, H., Formation, properties and high-temperature behaviour of mullite. Habiliationsschrift (thesis), Faculty of Chemistry, University of Münster, FRG, 1986, pp. 1–148.
15. Gelsdorf, G., Müller-Hesse, H. and Schwiete, H. E., Einlagerungsversuche von synthetischem mullit, und substitutionsversuche mit gaillumoxid and germaniumoxid, teil II. *Arch. Eisenhüttenwesen*, 1958, **29**, 513–519.
16. Schneider, H., Zirconium incorporation in mullite. *N. Jb. Min. Mh.*, 1986, **49**, 172–180.
17. Schneider, H., Solid solubility of Na_2O in mullite. *J. Am. Ceram. Soc.*, 1984, **67**(7), C130–131.
18. Razumovski, S. N., Tunik, T. A., Fisher, O. N. and Shmitt-Fogelvich, X-ray analysis of solid solution of ferric oxide in mullite. *Refractories*, 1977, **18**(1–2), 546–548.
19. Ford, W. E. and Rees, W. J., Mullite-chrome mixtures. *Trans. Brit. Ceram. Soc.*, 1946, **45**(3), 125–136.
20. Baudin, C., Osendi, M. I. and Moya, J. S., Solid solution of TiO_2 in mullite. *J. Mater. Sci. Lett.*, 1983, **2**(5), 185–187.
21. Schneider, H. and Rager, H., Occurrence of Ti^{3+} and Fe^{2+} in mullite. *J. Am. Ceram. Soc.*, 1984, **67**(11), C248–250.
22. Schneider, H. and Rager, H., Iron incorporation in mullite. *Ceram. Int.*, 1986, **12**(3), 117–125.
23. Schneider, H., Temperature-dependant iron solubility in mullite. *J. Am. Ceram. Soc.*, 1987, **70**(3), 43–45.
24. Cameron, W. E., Composition and cell dimensions of mullite. *Am. Ceram. Soc. Bull.*, 1977, **56**(11), 1003–1011.
25. Chaudhuri, S. P. and Patra, S. K., Preparation and characterisation of transition metal ion doped mullite. *Brit. Ceram. Trans.*, 1997, **96**(3), 105–111.
26. Brownell, W. E., Subsolidus relation between mullite and iron oxide. *J. Am. Ceram. Soc.*, 1958, **41**(6), 226–230.
27. Zimmermann, K. and Favejee, J. C. L., *Ber. Deut. Keram. Ges.*, 1941, **22**, 277.
28. Noble, W., 9th Clay Convention, Nat'l. Fed. Clay Indust. Edinburgh, 1949.
29. Noble, W., *Claycraft*, 1950, **23**, 482.
30. Claussen, N. S. and Jahn, J., Mechanical properties of sintered, in-situ reacted mullite-zirconia composites. *J. Am. Ceram. Soc.*, 1980, **63**(3/4), 228–229.
31. Ansean, M. R., Di rupo, E. and Cambier, F., Thermal expansion of zirconia–alumina materials prepared by reaction sintering. *J. Mater. Sci.*, 1981, **16**(3), 825–828.
32. Moya, J. S. and Osendi, M. I., Effect of ZrO_2 (SS) in mullite on the sintering and mechanical properties of mullite/ZrO_2 composites. *J. Mater. Sci. Lett.*, 1983, **2**(10), 599–601.
33. Kirillova, G. K., Elektrische eigenschaften Von mullit. *Keram. Z.*, 1959, **11**, 638–640.
34. Saalfeld, H. and Guse, W., Mullite and mullite matrix composites. In *Ceramic Transactions 6*, ed. S. Somiya, R. F. Davis and J. A. Pask. American Ceramic Society, Westerville, OH, 1990, pp. 73–101.
35. Sanyal, D., Patra, S. K., Chaudhuri, S. P., Gangiali, B. N., Banerjee, D., De, U. and Bhattacharya, R. L., Study of transition metal ion doped mullite by positron annihilation techniques. *J. Mater. Sci.*, 1996, **31**(13), 3447–3451.
36. Chaudhuri, S. P. and Patra, S. K., Electron paramagnetic resonance and mössbauer spectroscopy of transition metal ion doped mullite. *J. Mater. Sci.*, submitted for publication.
37. Schneider, H., Mullite and mullite matrix composits. In *Ceramic Transactions 6*, ed. S. Sōmiya, R. F. Davis and J. A. Pask. American Ceramic Society, Westerville, OH, 1990, pp. 135–157.
38. Schneider, H., Okada, K. and Pask, J. A., *Mullite and Mullite Ceramics*., John Wiley, London, 1994, p. 76.
39. Rager, H., Schneider, H. and Graetch, H., Chromiun incorporation in mullite. *Am. Min.*, 1990, **75**, 392–397.
40. Gerardin, C., Sunderasan, S., Benziger, J. and Novrotsky, A., *Chem. Mater.*, 1994, **6**, 160.
41. Anderson, J. C., Lever, K. D., Alexander, J. M. and Rawlings, R. D., *Materials Science*, 2nd edn., Thomas Nelson and Sons Ltd, Middlesex, 1977, pp. 315–340
42. Gilreath, E. S., *Fundamental Concepts of Inorganic Chemistry*. McGraw–Hill, New York, 1958 (Ch. 2).